ISSN (Online) 2394-2320

International Journal of Engineering Research in Computer Science and Engineering (IJERCSE)

Volume 11 Issue 08 August 2024

Development and Verification of a Wireless Charging Dock for Low-Cost Drones

[1] Brennen Barfuss, [2] Lalle M. N'diaye, [3] Ehsan Rohani, [4] Mohammad A.S. Masoum, [5] Mohammad Shekaramiz

[1][3][4][5] Electrical and Computer Engineering Department; Utah Valley University, Orem, USA
[2] PacifiCorp; American Fork, Orem, USA
Email: [1] 10706480@uvu.edu, [2] lalle.n'diaye@pacificorp.com, [3] ehsan.rohani@uvu.edu, [4] mmasoum@ieee.org, [5] mshekaramiz@uvu.edu

Abstract*— The autonomous operation of drones is becoming increasingly popular, with a growing demand to extend flight times for applications such as surveillance, tracking, and inspections. One of the most promising solutions for enhancing drone power autonomy is the use of docking stations. These stations facilitate landing and recharging, provide proximity to the work area, improve automation, and eliminate the need for user interaction. To address this need, we designed, prototyped, and tested an inductive charging system for wireless charging of small, low-cost drones. The constructed charging system consists of two main components: a portable dock housing with integrated power transmitting module, and the power receiving device. The receiver system connects to the drone onboard battery via an innovative landing gear attachment. We also investigated the efficiency of wireless power transfer at different transmitting frequencies and filter capacitances. Finally, we implemented the system for a DJI Mini 4 Pro drone to charge its DJI 3850 mAh Intelligent Flight Battery Plus, testing both energy transfer and landing capabilities. The constructed prototype achieved an output power of 26.7 W with a power transfer efficiency of 63.3% at a transmitting frequency of 200 kHz. Our investigation indicates the additional payload added by the receiving circuit reduces the drone's flight time, as expected.

***Index Terms*— Wireless Power Transfer, Drone, Wireless Charging, Dock Station, Inductive Power Transfer**

I. INTRODUCTION

The drone market is growing rapidly and is expected to reach nearly $100 billion by 2030 [1]. Huge growth in drone adoption is forecasted in the logistics, industrial, and agricultural sectors for a variety of tasks that require autonomous 24/7 operation such as monitoring and inspection of goods and assets, video surveillance, delivery, environmental mapping, etc. However, with today's technology, the battery charge of most drones varies from 5 to 60 minutes [1]. In most cases, when the drone reaches low power, it needs to land, and the battery is manually replaced. This process is inefficient and time-consuming. Furthermore, this is not suitable for the increasingly common autonomous operation of drones and requires a human operator on site. Two possible automatic approaches to extend drone battery power autonomy are being investigated and deployed:

- Battery swapping systems [1-3] that require high accuracy, precise positioning, and special design of batteries and battery compartments.
- Battery charging stations [1, 4-5] which are less complex than Battery swapping systems.

Battery charging stations are given more attention and divided into two main groups [4]:

1- Wired charging stations that have high power transfer efficiency.
2- Wireless charging stations that have lower power transfer efficiency but are more reliable in terms of energy transfer and environmental changes.

Wireless charging technology has been gaining popularity in recent years and is now commonly found in smartphones, smartwatches, and other electronic devices. The main challenge with wireless charging stations is the precise alignment of the transmitter and receiver coils after landing. They are classified into two main categories [1, 4]:

a) Wireless charging stations without landing positioning system that require a sophisticated drone control system to ensure the desired accuracy during landing.
b) Wireless charging stations with landing positioning system that can be divided into two main groups [1]: with active and passive positioning. Active positioning systems include actuators and mechanisms to adjust the position and orientation of the drone during landing [6-7]. Compared to passive positioning systems, these systems are more complex, less fail-safe, and require more time for the drone to reach the correct position. Passive positioning systems include funnels for one or for each leg, overhead funnels, and closed contours.

Drones with wireless charging can autonomously perform various tasks such as survey, surveillance, tracking, and inspections. However, this autonomy is disrupted when the drone's battery depletes. At this point, the user must halt operations to recharge the drone or replace its battery. This interruption is inconvenient as it requires the user to monitor the drone's battery charge state of charge.

Highlighting the importance of wireless charging for drones, some manufacturers are releasing commercial docking stations [1, 3]. However, these stations, like DJI

ISSN (Online) 2394-2320

International Journal of Engineering Research in Computer Science and Engineering (IJERCSE)

Volume 11 Issue 08 August 2024

Dock1 and Skydio Dock2 [1], are designed exclusively for their specific drones, which restricts their compatibility and scalability with other drone models. For instance, the DJI Dock 2 charging station, designed for the DJI Matrice 3D/3TD costs around $9,000. This paper aims to provide a solution suitable for small, affordable, commercial-sized drones.

Reference [8] proposes an automatic drone charging station using magnetic induction principle. The charger is made up of receiving and transmitting circuits. The receiver is attached to the bottom of the drone. The UAV can land freely on the station since it has a motorized system that will move the transmitter circuit to the bottom of the drone. To resolve the misalignment tolerance issue of the coils, a wireless charging system is developed in [9] with a squirrel cage receiver coil embedded in the landing gear of the drone and a circular transmitting coil design. The two transmitting coils are connected in series with a small transmitting coil at the concentric position of the main transmitting coil. For an 85 kHz square wave ac voltage from the transmitter circuit of the charger, the experiment results indicate that the dc–dc transmission efficiency of this system is 74%–80%. The output current obtained was 2.28 ± 0.32 A within a ±110 mm gap between the transmitter and receiver circuits. Reference [10] develops a 400 W wireless charging system prototype in 85 kHz band for overhead power transmission line patrol. The dc output average voltage is 47.2 V with an active power of 435 W and a system efficiency of 78%. The proposed prototype system is a low-cost wireless charging dock for small commercial drones aiming to enhance the autonomy of drones and their operational efficiency.

The main aims of this paper are as follows:

- Design, develop, prototype, and test an inductive charging system for wireless charging of small, low-cost drones. This system consists of a portable dock with rechargeable batteries that house the integrated power transmitting circuit and a power receiving circuit mounted on the drone with 3D-printed landing gear.
- Investigate the performance and efficiency of the designed wireless power transfer at different transmitting frequencies and with various transmitter and receiver filter capacitances.
- Implement and test the designed wireless charger using breadboard and perf board methods.
- Construct and test a prototype of the designed wireless charger for a DJI Mini 4 Pro drone to charge its DJI 3850 mAh Intelligent Flight Battery Plus.

In the remainder of this paper, the design and simulation of the wireless charger system is explained in Section II, the breadboard and perf board implementation and testing of designed transmitter and receiver circuits are presented in Section III followed by the prototyping of the final design and the conclusions in Sections IV and V.

II. DESIGN OF WIRELESS CHARGING SYSTEM

A. Block Diagram of Designed Wireless System

A portable source of power is desired for the transmitting side of the wireless charging system. This will enable the charging dock to be used when no utilities are available. Ideally the source needs to be rechargeable and able to hold enough power for multiple charging cycles across various days. Using various voltage regulators, a 12V battery can provide the necessary over-current protection and required voltages for the design. The Arduino Nano and logic gates require a 5V input, the MOSFET drivers require 12V to boost the signal to the desired amplitude and 15V to power DC-AC inverter. Each of these components will be discussed with further detail in the following sections.

Figure 1 illustrates the block diagrams of the designed transmitter and receiver charging system. Since the power source is DC, the design requires a conversion to AC to induce current from the transmitting coil to the receiving. The nature of wireless charging uses the properties of AC power transfer or otherwise will not function. To make DC-AC conversion a full sweep H-bridge inverter is used producing a high-power square wave. A full sinusoidal pulse width modulation (SPWM) signal would be ideal, however due to the frequency requirement it was decided that a square wave would suffice. Once the oscillating current is produced the design uses corresponding capacitors between the transmitter and receiver to produce a wave as close to a sine wave as possible. This is fed through the transmitting and receiving coils.

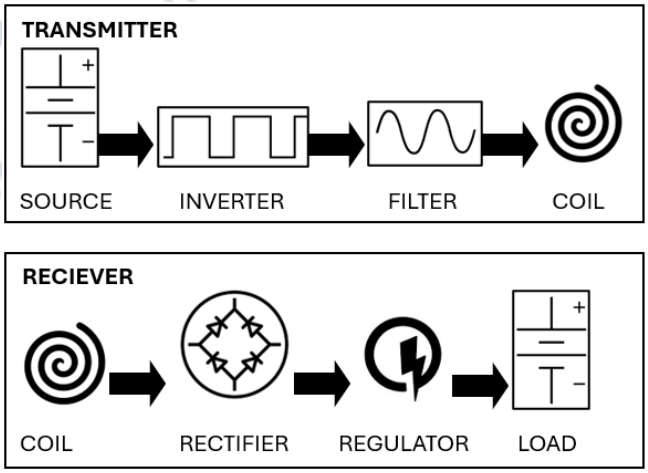

Fig. 1. Block diagrams of designed transmitter and receiver circuits.

Once the current is induced in the receiving coil, the load/battery requires a DC current. Hence, AC-DC power conversion is performed using a full-bridge rectifier circuit. To protect the load, a voltage regulator is also included before connecting to the USB type C port of the drone. However, as not foreseen during the simulations it is preferrable to use a fast-charging QC3.0 voltage regulator as this will allow the

ISSN (Online) 2394-2320

International Journal of Engineering Research in Computer Science and Engineering (IJERCSE)

Volume 11 Issue 08 August 2024

battery protection circuitry withing the drone to communicate with the wireless charging system. Without this feature, the load is unable to accept more than a 5W input.

B. Simulation of Designed Wireless System

Before any physical implementation of the design many variations of the wireless charging system were tested until the desired results were obtained. Figure 2 shows the simulation of the designed transmitter and receiver circuits in Multisim along with the waveforms of the H-bridge inverter input transmitting coil, and the corresponding output/load signals at 100kHz.

C. Impact of Coil Configuration and Frequency

Table 1 presents a sample of tests highlighting the effect of coil design with the corresponding capacitance and varying frequency. During these tests a 3 ohms resistor was used as load to emulate the drone battery and the input voltage was reduced to protect the circuit from potential overcurrent issues, resulting in lower output power. Various frequencies (not included in the table) were tested, with 200kHz proving optimal compared to the 100kHz used in the previous design shown in of Fig. 2a. The tests concluded that frequencies above 100kHz provided higher power up to 200kHz, beyond which the power output began to decline. Additionally, the tests showed that a larger diameter coil with more windings was more effective. A test with the coil ratio of 1:2 in windings to double the receiver output was also performed; however, it was found that the circuit was more efficient and stable when the coils had the same number of windings.

Table 1. Measured output power for different transmitter and receiver coils configurations and frequency.

Coil Configuration	100 kHz	200 kHz
Double coils, 270 nF compensation	2.89 W	4.84W
Large coils with 170 nF compensation	4 W	7.29 W
Single coils with 270 nF compensation	2.56 W	4.41 W
Single coils (transmitter) and double coils (receiver), 270 nF compensation	1.69 W	6.76W

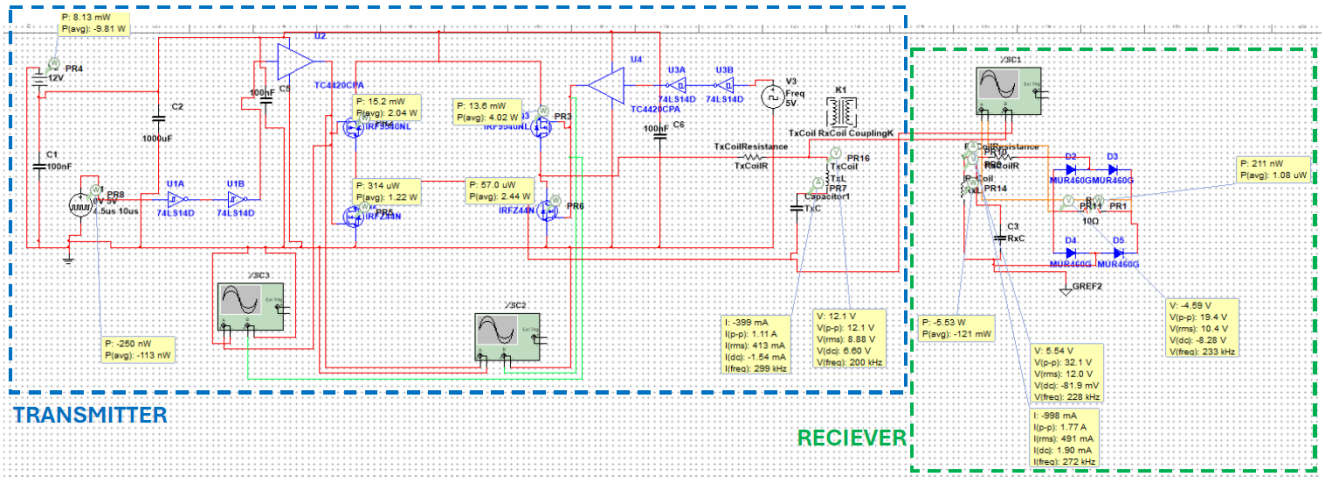

Fig. 2a. Schematic simulation of the designed transmitter and receiver circuits in Multisim.

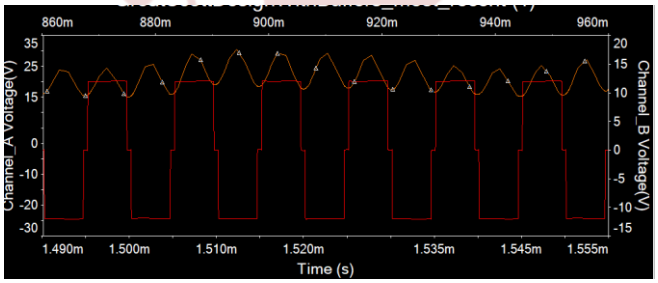

Fig. 2b. Waveforms of the H-bridge inverter input (Channel A, red) and the output/load (Channel B, orange) at 100kHz.

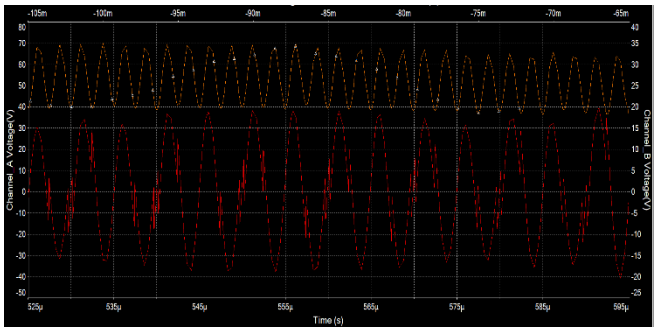

Fig. 2c. Waveforms of the Transmitting coil (Channel A, red) and output/load (Channel B, orange) at 100kHz.

ISSN (Online) 2394-2320

International Journal of Engineering Research in Computer Science and Engineering (IJERCSE)

Volume 11 Issue 08 August 2024

III. BREADBOARD/PERF BOARD IMPLEMENTATION AND TESTING OF DESIGNED WIRELESS SYSTEM

Once a successful simulation was achieved, initial evaluations and testing of the wireless system were conducted by breadboard and perf board implementations of the transmitting and receiving circuits, respectively.

A. Breadboard Implementation of Transmitting System

Figure 3 illustrates the breadboard implementation of the designed transmitting circuit. The first step for the implementation of the transmitting circuit is to convert the DC power from the battery source to AC power. This is done using a full sweep H-Bridge MOSFET inverter. During simulation it was learnt that a full H-bridge proved to be more effective than a half bride driver. The H-bridge inverter requires two signals to drive each side of the inverter. Each signal feeds a MOSFET N-channel and P-channel pair. When one pair is activated, it causes current to travel in one direction and the other pair in the opposite direction creating the oscillating current. However, it is vital that neither pair can be activated at the same time. To accomplish this, a section of the design is dedicated protection to provide opposing square wave signals that cannot provide a high signal concurrently. This design is shown in Fig. 3a. Note the application of Arduino and logic gates in Fig. 3a instead of the function generator used in the simulations (Fig. 2a).

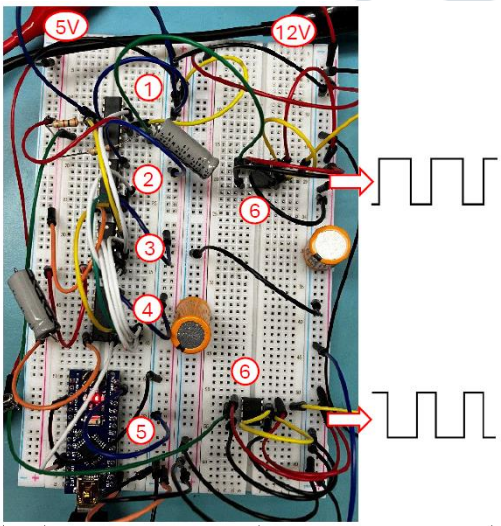

1	LM339N	COMPARATOR
2	SN74LS86SN	XOR GATE
3	SN74LS08N	AND GATE
4	SN74LS04N	NOT GATE
5	A000005	ARDUNINO NANO
6	TC4420CPA	MOSFET DRIVER

Fig. 3a. Breadboard implementation and testing of transmitter; Part 1: Generation of two complementary square waves for the inverter.

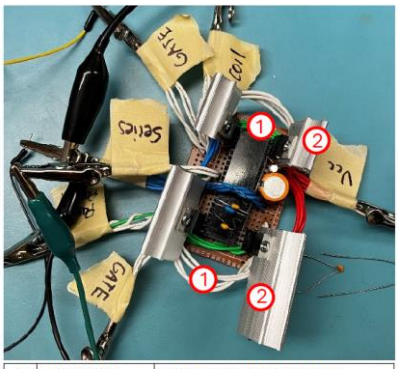

1	IRFZ44N	MOSFET N-CHANNEL
2	IRF9Z34N	MOSFET P-CHANNEL

Fig. 3b. Perf board testing of transmitter; Part 2: Full bridge inverter.

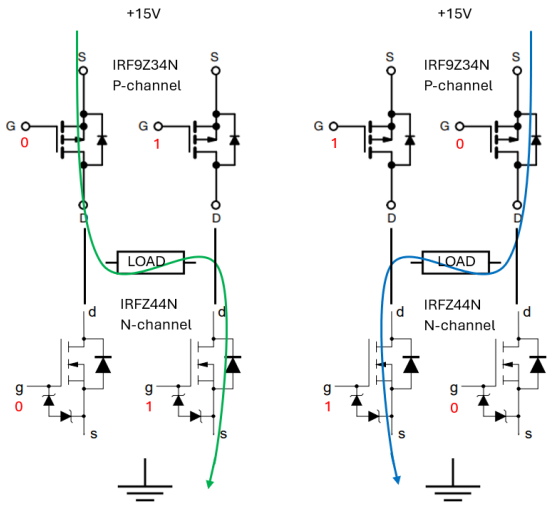

Fig. 4. H-bridge inverter schematic diagram.

Following are analyses of the transmitter circuit (Fig. 3):

- An Arduino Nano is used to generate a 5V amplitude 200kHz square wave signal. This signal is then passed through a series of logic gates beginning with an inverting NOT gate to provide an opposing signal. Followed is an XOR Gate which takes both signals as inputs and outputs only sections of the two signals at which they are not high at the same time. This output is then fed through an AND gate with the original signal and inverted signal eliminating the possibility of triggering both sides of the H-bridge at the same time. For extra precaution a comparator is also used to provide additional control of the time spacing between each signal. Comparing the signal to the 3.3V source of the Arduino provided a convenient and comfortable separation between each signal.
- The generated signal has a small amplitude of 5V max due to the limitations of the Arduino Nano while the gates of the MOSFETS require a higher voltage to accommodate for the 15V provided to the inverter. To accomplish this a pair of MOSFET drivers are used as seen in Fig. 3a with the TC4420CPA amplifying the square wave signals to an

ISSN (Online) 2394-2320

International Journal of Engineering Research in Computer Science and Engineering (IJERCSE)

Volume 11 Issue 08 August 2024

amplitude of 12V.

- The two square wave signals are the full H-bridge MOSFET inverter/driver as shown in Fig. 3b. This section of the circuit was completed using a perf board due to high ampacity of the circuit to reach 4A. Multiple wires were used for each connection to account for the high frequency and current. During previous trials it was deemed necessary to have individual heat sinks for each MOSFET.
- The original square wave signal provides a signal to a P-type/N-type MOSFET pair creating one side of the bridge causing the current to pass through the load in one direction. The inverted square wave provides a signal to the other P-type/N-type MOSFET pair causing the current to pass through the load (coil) in the opposite direction as seen in Fig. 4. This switching is 200kHz which was tested to be the optimal frequency for the designed system.
- The gate/MOSFET driver used in the circuits of Fig. 2a and 3a is the TC4420PA. It features a latch-up protection that can withstand >1.5A and a reverse output current.
- The full bridge inverter used in the transmitter circuits is made up of P-channel MOSFETs (IR9Z34N, Figs. 3b) and N-channel MOSFETs (IRFZ44N, Figs. 2a and 3b).
- The IR93Z4N used in the circuits of Figs. 3b has the following specification: 1) A drain Current –I D=-19A@ TC=25℃, 2) A drain Source Voltage-V DSS=- 55V, 3) A static Drain-Source On-Resistance RDS (on) = 0.1Ω, and 4) Fast Switching properties.

The inverter can provide an oscillating current through the load (coil); however, the output is a square wave. To achieve the high efficiency, the current passing through the load needs to be as close to a sinusoidal wave as possible. Therefore, a filter is applied to the design containing a capacitor pair on each side of both the transmitter and receiver circuits (Figs. 3-5). Each capacitor is placed in series with the coil which proved to be potentially more efficient/effective than parallel and hybrid configurations. Under ideal sinusoidal operating conditions, the optimal value of the filter capacitor, C, at the resonant frequency can be calculated using the formula $C=1/[L*(2\pi f)^2]$ where L is the circuit inductance and f is the frequency [11]. The optimal capacitance value was calculated to be 170nF for our filter design. However, during the implementation under non-ideal and non-sinusoidal operating conditions, the capacitance value was optimized during the prototype testing stage of the project as explained in the following section.

B. Perf Board Implementation of Receiver System

Once the power is transferred to the receiving coil with adequate filtering, the produced current flow then needs to be converted to DC. The Lithium Ion in the drone battery requires a DC current for charging. This conversion is performed by a full bridge rectifier and filtering capacitor. Due to the expected high power, this section of the circuit was also implemented using a perf board. As explained previously, the drone does have battery protection circuitry of its own; however, having the receiver connected directly to the drone via USB type C was not able to push current to the load/battery. A QC3.0 fast charging voltage regulator was then used in series with the receiver to provide the necessary voltage and current to the drone. Figure 5 shows the perf board implementation of the designed receiving circuit.

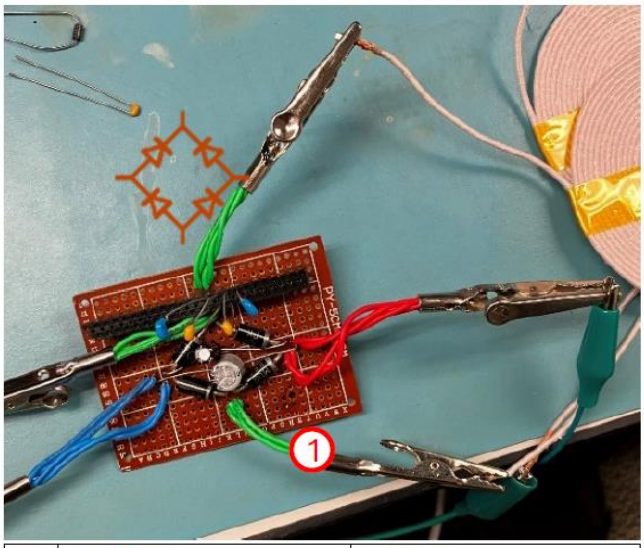

1	MUR460	DIODE

Fig. 5. Pref board implementation and testing of the receiver.

C. Testing of Transmitter and Receiver Circuits

The testing of implemented circuits involved confirming the power transfer between the transmitting and receiving coils, assuring power delivery to the actual load, and determining the transfer efficiency between the charger and the load. An inline USB type C digital multimeter as seen in Fig. 6 is used to display the voltage, current, and power delivered to the battery during testing. The drone battery charger power specified by the manufacturer is 30W while the measured off-wall power is only 28.38W (Fig. 6). This difference between the off-wall power (28.34W) and the implemented circuit power (23.38W) may be due to the initial charge of the drone battery at the time of the measurement.

IV. PROTOTYPING OF DESIGNED WIRELESS CHARGER

After completing the breadboard and perf board testing of the transmitting and receiving circuits, the overall wireless charger system was modeled into a PCB [12].

A. PCB Design: Transmitter

Fig. 7a shows the schematics of the transmitter prototype. The transmitter PCB layout as seen in Fig. 7b highlights differences compared to the schematic as the actual sizes of the components are required. The analog part of the circuit

ISSN (Online) 2394-2320

International Journal of Engineering Research in Computer Science and Engineering (IJERCSE)

Volume 11 Issue 08 August 2024

generating the desired square wave has a smaller trace width compared to the inverting part for current carrying capacity. The blue and red traces represent the different bottom layers of the PCB. The final component layer of the PCB can be seen in Fig 7c while the assembled transmitted circuit is displayed in Fig 7d.

Off-Wall and Wireless Charging Test Results		
Measured Prameter	Off-Wall Testing	Breadboard and Pref Board Testing
Input Voltage	Not Measured	15V
Input Current	Not Measured	2.45A
Input Power	Not Measured	36.75W
Output Voltage	11.80V	11.23V
Output Current	2.40A	2.082A
Output Power	28.34W	23.38W
Efficiency	NA	63.6%

Fig. 6. Results of breadboard testing (Figs. 3 and 5).

The JLC PCB and EasyEDA were used to design and order the PCB. The process starts by first laying out the schematic followed by designing the PCB trace layout as shown in Fig. 7b. The square wave signal generator and H-bridge inverter were designed into one PCB. A trace width of 6mm was used for the high-power inverter side of the transmitting circuit which is double the calculated required width. However, during testing this trace width was proven insufficient requiring additional modifications to the PCB. It is suspected that the high frequency of the circuit is the reason the system required a larger trace width. As seen in the schematic, additional capacitor slots and holes for the coils were included to provide flexibility for adjusting the filtering aspect of the design as needed to optimize the circuit design.

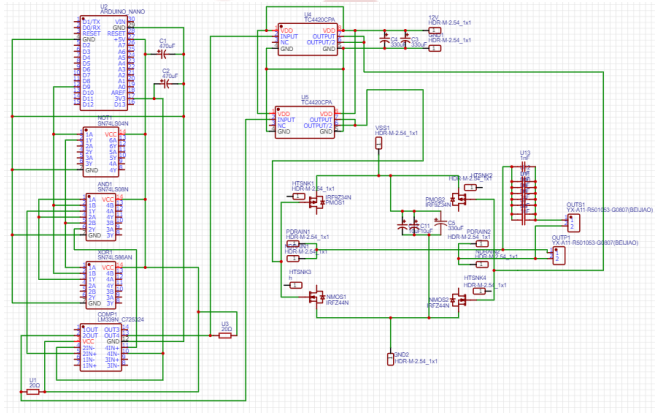

Fig. 7a. Schematic of constructed transmitter prototype.

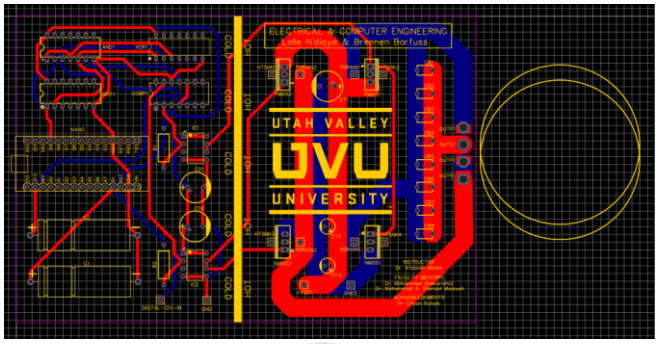

Fig. 7b. PCB layout of the constructed transmitter.

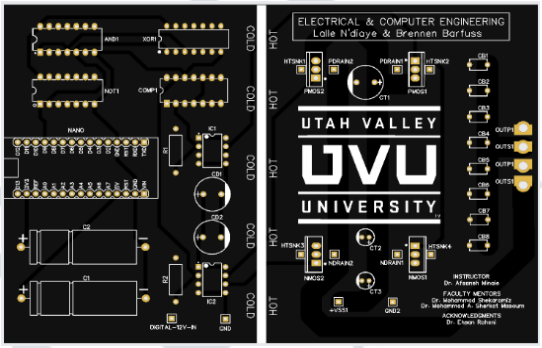

Fig. 7c. Final PCB of the constructed transmitter.

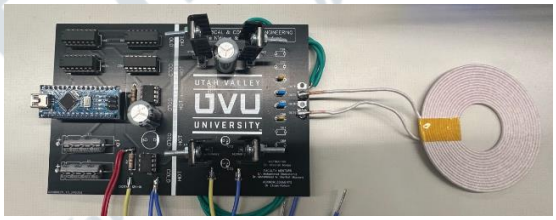

Fig. 7d. Constructed prototype of the transmitter.

B. PCB Design: Receiver

Fig. 8a shows the schematic of the receiving prototype. Fig. 8b displays PCB layout of the constructed receiver. The final component layer of the receiver circuit can be seen in Fig 8c. The receiver prototype was then assembled as seen in Fig. 8d.

Since the receiver circuit is attached to the drone, the PCB was designed to be as small as possible to reduce the weight.

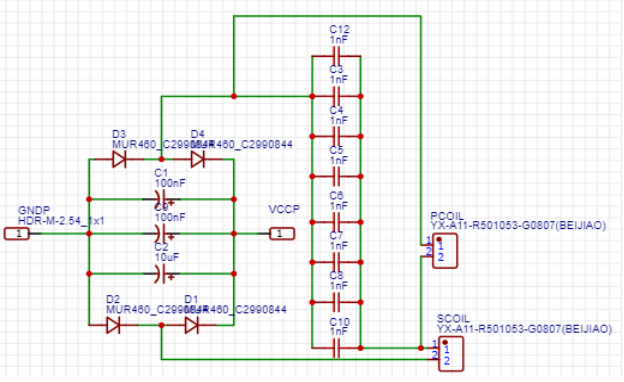

Fig. 8a. Schematic diagram of constructed receiver prototype.

ISSN (Online) 2394-2320

International Journal of Engineering Research in Computer Science and Engineering (IJERCSE)

Volume 11 Issue 08 August 2024

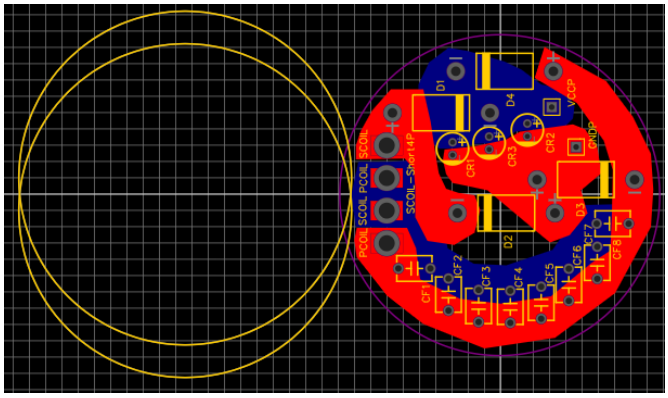

Fig. 8b. PCB layout of the constructed receiver.

C. 3-D Modeling of Landing Gear

The landing gear became a crucial component of the project. To minimize any impact on the drone's flight capabilities, a design that was both sturdy and lightweight was required. As shown in Fig. 9, the landing gear features a top attachment that clips onto the drone and a supporting plate that hooks onto the legs of the attachment. The plate is hollow and includes circular clips at its center to hold the receiving circuit and receiving coil.

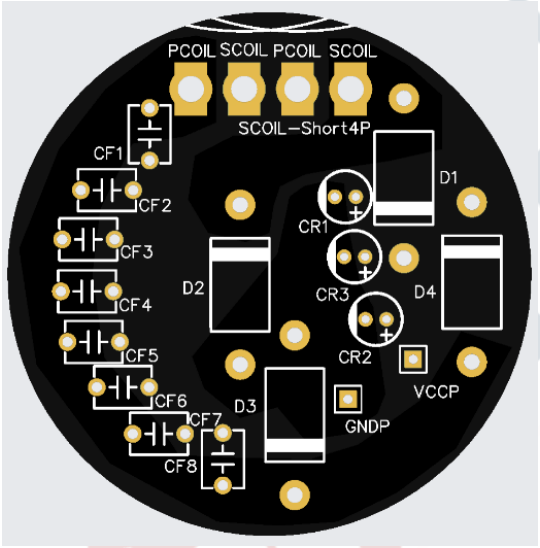

Fig. 8c. Final PCB of the constructed receiver.

Fig. 8d. Constructed prototype of the receiver.

Another aspect that drastically changed the design of the landing gear is the omnidirectional sensors on the drone. If any part of the gear was to block the bottom sensor the drone would mistake it as the ground and cause continual upward flight. For this reason, the receiving coil and circuit is mounted towards the back of the landing gear out of the angle of vision of the bottom sensors. The receiving circuit is also mounted on legs a few centimeters below the drone as to avoid blocking the cooling air vents for the battery and to lift the level of the blades to avoid collision with the docking station. The legs are in an open delta arrangement to help off balance the additional weight added by the receiving circuit. Due to bounce in the legs additional support were added along with an oval shape to the tubular shafts to help reduce any vertical flexibility. Designed for minimal weight the landing gear was also printed using a carbon fiber PLA material as shown in Fig. 9.

Fig. 9. Construction of the landing gear using 3D printer.

D. Impact of Filter Capacitance and Prototype Testing

Before constructing the prototype of the designed wireless charging system, the impact of transmitter and receiver filter capacitances on the performance and output of the wireless charger was investigated. Table 2 presents a sample of tests highlighting the effects of filter capacitance on the wireless charger's output power. Five filtering scenarios at a frequency of 200 kHz were tested. The tests concluded that transmitter and receiver filter capacitances of 170 nF and 570 nF, respectively, resulted in better sinusoidal operating conditions with less harmonic distortion and higher output power, as indicated in row 4 of Table 2.

The constructed prototype of the designed wireless charging dock for low-cost drones is shown in Fig. 10. Various charging scenarios with different drone battery states of charge were tested. Table 3 shows the performance of the constructed prototype for a sample drone wireless charging scenario, achieving an efficiency of 63.3%.

ISSN (Online) 2394-2320

International Journal of Engineering Research in Computer Science and Engineering (IJERCSE)

Volume 11 Issue 08 August 2024

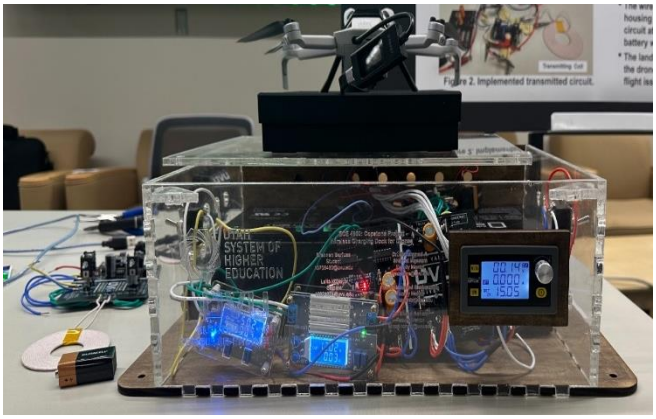

Fig. 10. The constructed wireless charging prototype achieving an output power of 26.7 W with an efficiency 63.3% at 200kHz.

Table 2. Impact of transmitter and receiver filter capacitance on the output power of the wireless charger at 200 kHz.

Transmitter Filter Capacitance	Receiver Filter Capacitance	Output Power
170 nF	170 nF	15 W
270 nF	270 nF	20 W
170 nF*	**570 nF***	**25.5 W**
170 nF	270 nF	19 W
160 nF	270 nF	21.6 W

*) Filter specifications used in the constructed prototype of Fig. 10.

Table 3. Prototype test results for a typical drone battery charging scenario (Fig. 10).

Input Voltage, Current, Power	15 V, 2.81 A, 42.15 W
Output Voltage, Current, Power	11.3 V, 2.36 A, 26.7 W
Constructed Prototype Efficiency	63.3%

V. CONCLUSIONS

This paper presents the design, development, and prototyping of an inductive wireless charging dock for small, low-cost drones. The charging capabilities of the proposed wireless docking station were tested on a DJI Mini 4 Pro drone, specifically targeting its DJI 3850 mAh Intelligent Flight Battery Plus.

The research was executed in three stages: 1) research and simulations, 2) implementation and testing using breadboard and perf board methods, and 3) prototyping and PCB design. Initially, various wireless charging designs were researched, and their capabilities tested using NI Multisim software. Motor driver circuits were also examined to better understand the principles of wireless charging. A combination of different designs was then physically implemented and tested using a high-power 200W load resistor. Key outcomes and conclusions include:

- The constructed charging system features a portable dock that houses the integrated power transmitting module and a power receiving system connected to the drone battery via an innovative landing gear attachment.
- The final circuit design incorporates an H-bridge inverter, MOSFET drivers, filtering capacitors, wireless charging coils, and a full-bridge rectifier.
- The constructed breadboard and perf board transmitter and receiver circuits (Figs. 3-5) achieved an output power of 23.38 W with a power transfer efficiency of 63.6% at a transmitting frequency of 200 kHz (Fig. 6).
- Using the full sweep inverter, the constructed prototype system (Figs. 7-10) achieved an output power of 26.7 W with a power transfer efficiency of 63.3% at a transmitting frequency of 200 kHz (Table 3).
- It was observed that the additional payload from the receiving system reduces the drone's flight time.

Future work will focus on further enhancing the charging system to automatically recognize when the drone is running low on charge, precisely allocate the charging dock for landing, and detect when the charging process is complete.

ACKNOWLEDGMENTS

This work is supported by the Smith College of Engineering & Technology at Utah Valley University, funded through engineering initiative grants provided by the State of Utah and the Office of the Commissioner of Utah System of Higher Education (USHE)- Deep Technology Initiative Grant 20210016UT.

REFERENCES

[1] D. Stuhne, G. Vasiljevic, S. Bogdan and Z. Kovacic, “Design and Validation of a Wireless Drone Docking Station”, in 2023 International Conference on Unmanned Aircraft Systems (ICUAS), pp. 652-657, 2023.

[2] E. Barrett, M. Reiling, S. Mirhassani, R. Meijering, J. Jager, N. Mimmo, F.Callegati, L. Marconi, R. Carloni, and S. Stramigioli, “Autonomous Battery Exchange of UAVS with a Mobile Ground Base,” in 2018 IEEE International Conference on Robotics and Automation (ICRA), pp. 699–705, 2018.

[3] S. C. De Silva, M. Phlernjai, S. Rianmora, and P. Ratsamee, “Inverted Docking Station: A Conceptual Design for a Battery-Swapping Platform for Quadrotor UAVS,” Drones, vol. 6, no. 3, 2022.

[4] H. Ucgun, U. Yuzgec, and C. Bayilmis, “A Review on Applications of Rotary-Wing Unmanned Aerial Vehicle Charging Stations,” International Journal of Advanced Robotic Systems, vol. 18, 2021.

[5] M. Galimov, R. Fedorenko, and A. Klimchik, “UAV Positioning Mechanisms in Landing Stations: Classification and Engineering Design Review,” Sensors, vol. 20, no. 13, 2020.

[6] A. Rohan, M. Rabah, F. Asghar, M. Talha, and S. H. Kim, “Advanced Drone Battery Charging System,” Journal of Electrical Engineering and Technology, vol. 14, 2019.

[7] C. H. Choi, H. J. Jang, S. G. Lim, H. C. Lim, S. H. Cho, and I. Gaponov, “Automatic Wireless Drone Charging Station

Creating Essential Environment for Continuous Drone Operation," in 2016 International Conference on Control, Automation and Information Sciences, pp. 132–136, 2016.

[8] C. H. Choi, H. J. Jang, S. G. Lim, H. C. Lim, S. H. Cho and I. Gaponov, "Automatic Wireless Drone Charging Station Creating Essential Environment for Continuous Drone Operation", 2016 International Conference on Control, Automation and Information Sciences, Ansan, Korea (South), 2016, pp. 132-136, doi: 10.1109/ICCAIS.2016.7822448.

[9] P. Cao et al., "Embedded Lightweight Squirrel-Cage Receiver Coil for Drone Misalignment-Tolerant Wireless Charging", in IEEE Transactions on Power Electronics, vol. 38, no. 3, pp. 2884-2888, March 2023, doi: 10.1109/TPEL.2022.3225307.

[10] S. Obayashi et al., "400-W UAV/Drone Inductive Charging System Prototyped for Overhead Power Transmission Line Patrol", 2021 IEEE Wireless Power Transfer Conference (WPTC), San Diego, CA, USA, 2021, pp. 1-3, doi: 10.1109/WPTC51349.2021.9458215.

[11] W. Xie and K. Smedley, "General Full-Range Regulation Method for Resonant Switched-Capacitor Converters", 2022 IEEE International Power Electronics and Application Conference and Exposition (PEAC), Guangdong, China, 2022, pp. 1025-1029, doi: 10.1109/PEAC56338.2022.9959494.

[12] PCB Prototype & PCB Fabrication Manufacturer - JLCPCB, Jlcpcb.com, 2020. https://jlcpcb.com/